



COMPARISON OF THE FRETTING CORROSION CURRENT OF TWO COMMERCIAL MODULAR HIP IMPLANTS SUBJECTED TO DIFFERENT LEVELS OF MECHANICAL LOADING AND CYCLING FREQUENCY

Carvalho, S.S.¹, dos Santos, C.T.^{1*}, Cavalleiro, M.R.²,
Monteiro, A.R.D.², dos Santos, V.O.^{1,3}, Fernandes, W.G.¹

1 - Instituto Nacional de Tecnologia (INT) - Divisão de Materiais (DIMAT), Laboratório de
Caracterização de Propriedades Mecânicas e Microestruturais (LACPM).

Av. Venezuela, 82, Saúde, Rio de Janeiro/RJ.

2 - Universidade Federal Fluminense (UFF) - Departamento de Engenharia Química e de
Petróleo. Rua Passo da Pátria, 156, São Domingos, Niterói/RJ.

3 - Universidade Federal do Rio de Janeiro, Programa de Engenharia Metalúrgica e de
Materiais/COPPE, Cidade Universitária, Rio de Janeiro/RJ.

*claudio.santos@int.gov.br

ABSTRACT

Modularity in hip implants creates surfaces susceptible to micromovements, promoting tribocorrosion and the release of debris, which may lead to implant failure. The present study compares two commercial modular hip implants under fretting corrosion testing: one with an ASTM F1586 stainless steel stem and a Co-28Cr-6Mo head, and the other with an ASTM F1586 stainless steel stem and an ASTM F138 stainless steel head. Sinusoidal cyclic loading was applied at forces of 0.8 and 3.6 kN with frequencies of 1.0 and 3.0 Hz, with current measured by electrochemical method. In both implants, fretting corrosion increased with higher loads from 0.8 kN to 3.6 kN at both 1 and 3 Hz frequencies. The measured currents were higher for the implant composed of dissimilar alloys, despite its greater hardness and corrosion resistance. Thus, combining dissimilar alloys can enhance fretting corrosion due to the galvanic effect, emphasizing the need to avoid such combinations in modular implants.

Keywords: Debris, micromovement, tribocorrosion, electrochemical method, galvanic effect.

1. INTRODUCTION

Hip osteoarthritis is one of the leading causes of disability worldwide, affecting more than 500 million people (1). The articulating joint cartilage destruction leads to pain, joint stiffness, muscle dysfunction, impairment of gait, which may evolve to functional limitation and even disability of the hip joint (2, 3). Total Hip Arthroplasty (THA) is one of the most common surgical procedures treatments to decrease pain, improve function and enhance quality of life for patients with severe hip disease (4).

Modular hip implants have become widely used because they allow for better adaptation to the patient's anatomy, providing surgeons with several advantages, such as the ability to control the femoral head's position relative to the stem, use femoral heads with different diameters for the same stem, and employ different materials for the stem and femoral head (5). However, the modularity generates surfaces susceptible to micromovements and thus facilitate occurrence of tribocorrosion. The wear and the release of metal debris can lead to implant failure due to various factors such: intense pain, inflammatory reactions, pseudo-tumors, and others (6, 8). Therefore, it is imperative that the release of tribocorrosion debris and metal ions may be kept to a minimum.

In the case of cemented stems and heads, cobalt-chromium alloys (CoCr) are used because they offer greater wear resistance and higher corrosion resistance compared to the same components made from austenitic stainless steels (9). These properties can be useful in reducing the effects of tribocorrosion. Additionally, CoCr heads are sometimes chosen because they can reduce the wear of the polymeric acetabular component in hip prostheses. As a result, surgeons also prefer the combination of implants with dissimilar materials (10).

For THA implants, studies of tribocorrosion focus on the region of contact between the stem and head, where the trunnion is the part of the stem that connects with the head. Additionally, adverse tissue reactions to metal debris from this region are known as trunnionosis (11). The breakdown of the passive oxide layer during cyclic loading can generate metal ions and debris. Thus, fretting-corrosion testing with electrochemical analysis allows for real-time monitoring of the breakdown behavior of the passive oxide layer during testing (12).

The present study aims to compare the effects of varying loading and cycling frequency conditions on the fretting corrosion current in the contact region between

the head and stem of two commercial modular hip implants composed of different alloys and subjected to accelerated fretting corrosion testing. It is worth noting that there are few studies in the literature that evaluate the effect of mechanical loading levels and frequency on the fretting corrosion of hip implants. No studies were found that, together with the effect of load and frequency, also evaluate the effect of the difference between the materials of the implant components.

2. MATERIALS AND METHODS

2.1. IMPLANTS

In the present study, two cemented hip implants from different manufacturers were evaluated, both consisting of modular parts, stem and head, as shown in Figure 1. The first implant (Group 1), has femoral stem of high-nitrogen austenitic stainless steel (ASTM F1586), which will be referred as HNSS, and head of Co-28Cr-6Mo alloy (ASTM F1537), which will be referred as CoCr. The second implant (Group 2), also has HNSS stem and an austenitic stainless steel head (ASTM F138), referred as SS. Table 1 shows the chemical composition of the alloys for the stem and head, both for Groups 1 and 2. The femoral heads used have a diameter of 28 mm and a head bore of 12/14 mm. Both femoral stems can be classified as follows: double taper; collarless polished tapers; polished body; offset of 37.5 mm; stem length of 130 mm; stem angle of 135°; and trunnion 12/14 mm.

Figure 1. Commercial implants tested in this study: (a) Group 1 and (b) Group 2.

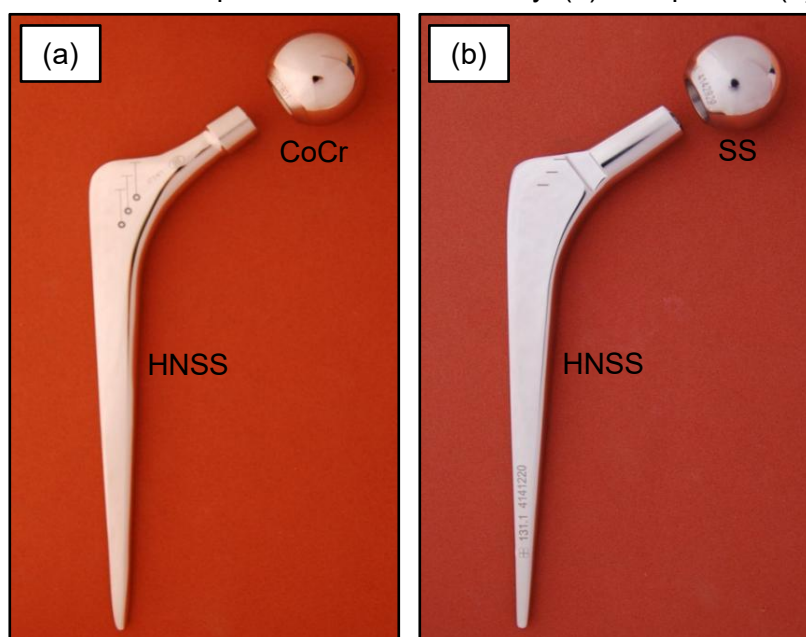


Table 1. Chemical composition (wt.%) by optical emission spectroscopy, combustion with infrared detection (C and S) and melting with thermal conductivity detection (N).

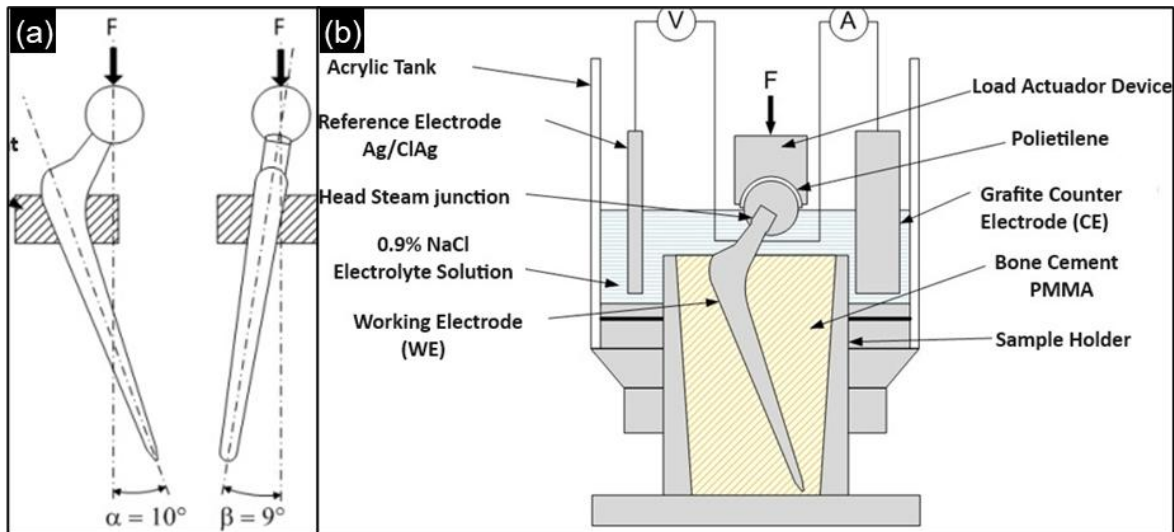
Element	Group 1		Group 2	
	Stem/F1586 (HNSS)	Head/F1537 (CoCr)	Stem/F1586 (HNSS)	Head/F1537 (SS)
C	0.038 ± 0.004	0.047 ± 0.004	0.043 ± 0.007	0.016 ± 0.001
Mn	4.01 ± 0.05	0.76 ± 0.08	3.83 ± 0.02	1.70 ± 0.05
Si	0.43 ± 0.02	0.45 ± 0.04	0.14 ± 0.03	0.37 ± 0.05
P	0.020 ± 0.001	-	0.009 ± 0.002	0.016 ± 0.001
S	<0.001	-	0.002	<0.001
Cr	19.5 ± 0.4	29.0 ± 0.7	19.5 ± 0.4	17.4 ± 0.3
Ni	9.3 ± 0.4	<0.1	9.8 ± 0.5	14.6 ± 0.5
Mo	2.0 ± 0.2	5.7 ± 0.2	2.31 ± 0.1	2.8 ± 0.1
Cu	0.07 ± 0.01	-	0.036 ± 0.00	0.10 ± 0.01
N	0.42 ± 0.01	0.177 ± 0.007	0.33 ± 0.02	0.079 ± 0.004
Nb	0.33 ± 0.06	-	0.33 ± 0.06	-
Fe	Balance	0.46 ± 0.12	Balance	Balance
Co	-	Balance	-	-

2.2. TESTING ASSEMBLING

The working electrode samples (Group 1 and 2) were prepared in accordance with the ASTM F1875 (or ABNT NBR ISO 7206-6) standard, embedded in bone cement (Polymethyl Methacrylate - PPMA) positioned with angles α and β equal to 10° and 9° , respectively (see Figure 2a). A conductive wire was fixed at the stem in order to be connected to the potentiostat.

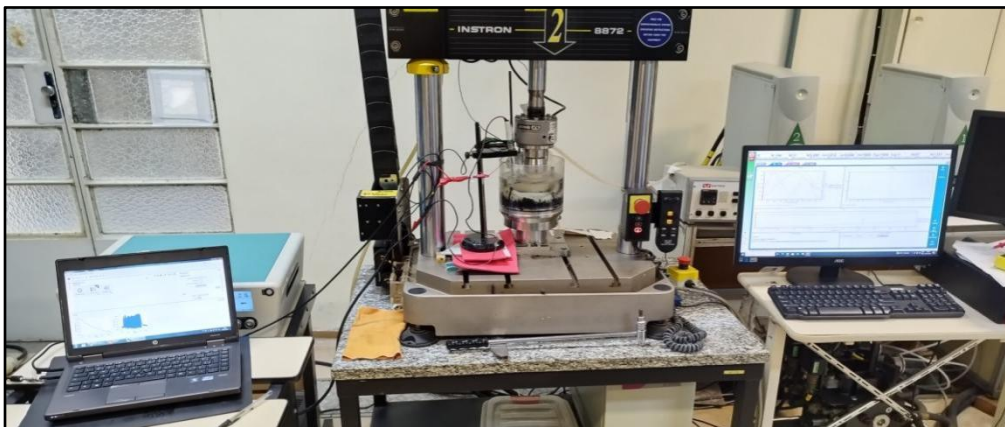
The electrochemical cell was prepared in a cylindrical acrylic tank where the metal parts have been previously insulated with insulating paint and then filled with approximately 2 L of 0.90% NaCl aqueous solution. The interface between the bone cement and the femoral stem was isolated from contact with the saline solution using silicone. The 3 electrodes of the electrochemical cell were assembled with Ag/AgCl as reference electrode, a graphite bar as counter electrode and the modular prosthesis (to be tested) as working electrode (see Figure 2b).

Figure 2. Implant positioning according to ASTM F1875 (a), and drawing of the electrochemical cell for fretting corrosion test of hip implants (b).



The electrodes were connected to a potentiostat (Metrohm model Autolab PGSTAT302N) and positioned at a Servo-hydraulic Fatigue Test machine (Instron model 8872) which was used to apply the mechanical loading to the hip implants. The apparatus was assembled as showed in Figure 3.

Figure 3. Experimental apparatus.



Procedures of tests were created in the software Nova 2.1 to be adapted for each condition. In this way, each data reading was sensitive to evaluate how the frequency of cycling or loading parameters was affecting the fretting corrosion process (in both Groups). The tests conditions were determined based on *Design of Experiments* (DoE), using 2^2 factorial design without replicas, including 3 central points to estimate residuals and pure error. The levels are shown at Table 2, which

were chosen considering that the normal human gait has a frequency between 1 and 2 Hz, and also the recommendation of the ASTM F1875 standard for electrochemical method of fretting corrosion analysis (frequency of 1 Hz, a maximum compression load of 2.040 kN and using $R = 0.1$). Frequencies and loads greater than 3 Hz and compression load of 3.6 kN, respectively, have not been studied. Hence, tests conditions are showed at Table 3.

Table 2. Parameters levels.

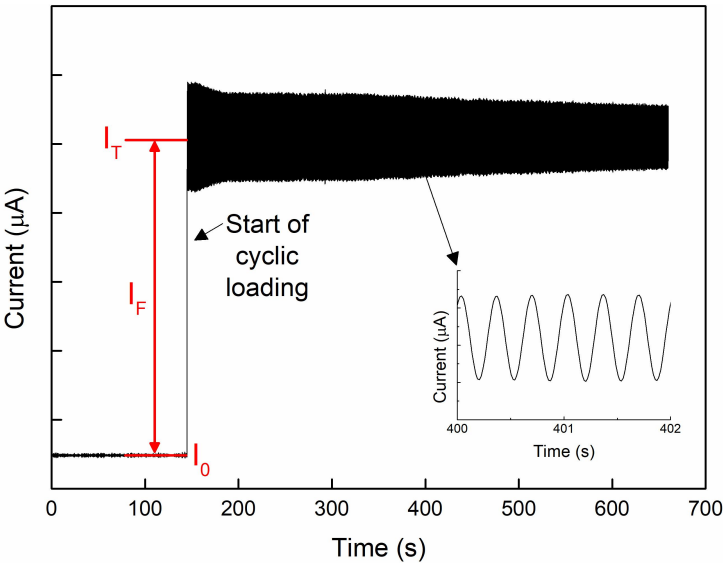
Parameter	Min	Max
Frequency (Hz)	1.0	3.0
Load (kN)	0.8	3.6

Table 3. Test condition design. Central points in bold.

Test N°	Load (kN)	Frequency (Hz)
1	0.8	1.0
2	3.6	1.0
3	0.8	3.0
4	3.6	3.0
5	2.2	2.0
6	2.2	2.0
7	2.2	2.0

The accelerated fretting corrosion test was adapted from the instructions of the ASTM F1875 standard in order to simulate (in the laboratory) conditions similar to those subjected to prostheses implanted in the human body. The corrosion current was monitored in stationary condition during 5 min. Then applying a cyclic sinusoidal load to the femoral head of the prosthesis for 10 minutes, followed by the stationary condition again during more 5 minutes. Then the fretting corrosion current (I_F) were calculated subtracting the average of the stationary corrosion (I_0) from the root mean square of the total corrosion (I_T) according to Figure 4.

Figure 4. Methodology used to calculate the fretting corrosion current (I_F).

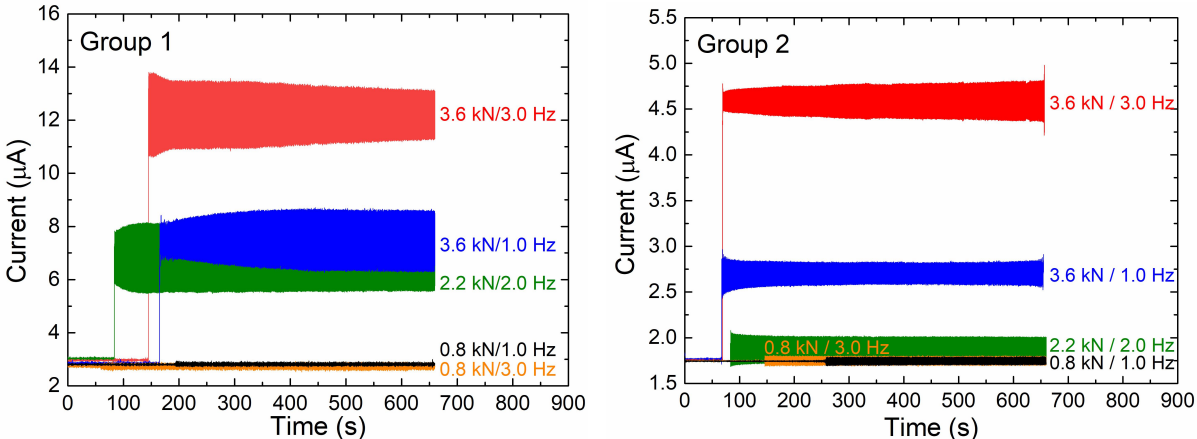


To reduce noise from other sources in the current versus time results, after the tests, some frequencies were filtered using the Fourier transform function (FFT). A band-pass FFT filter was used with cutoff frequencies of 0.5 - 2.0 Hz for tests carried out on loading frequency of 1.0 Hz, cutoff of 1.0 - 3.0 Hz on frequency of 2.0 Hz and cutoff of 2.0 - 4.0 Hz on frequency of 3.0 Hz.

3. RESULTS AND DISCUSSION

The following graphs (Figure 5) show the current profile measured under several condition tests of the Groups 1 and 2. All tests conducted within groups showed nearly the same value of stationary current (I_0). Therefore, there was minimal or negligible influence of the total current (I_T) in I_0 measured in subsequent tests on the same Group. For both groups, the I_T increased at the beginning of the loading cycles, except for the test with 0.8 kN. Additionally, when a cyclic load of 2.2 or 3.6 kN was applied, the Group 1 exhibited a higher value of I_T compared to Group 2.

Figure 5. Current profiles for the levels Min/Max and one Central Point for each group.



The summarized results of fretting corrosion ($I_F = I_T - I_0$) are displayed in Table 4.

Table 4. Fretting corrosion current for the levels Min/Max and Central Points (in bold).

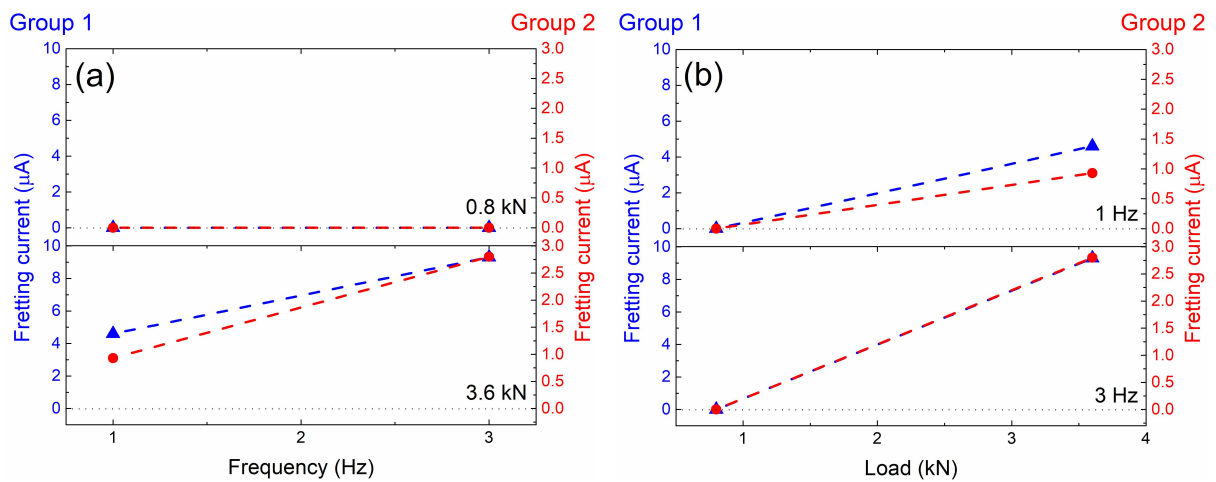
Test N°	Load (kN)	Freq. (Hz)	Group 1	Group 2
			I _F (µA)	I _F (µA)
1	0.8	1.0	0.00 ± 0.07	0.00 ± 0.03
2	3.6	1.0	4.6 ± 0.7	0.9 ± 0.1
3	0.8	3.0	0.0 ± 0.1	0.00 ± 0.03
4	3.6	3.0	9.3 ± 0.8	2.8 ± 0.1
5	2.2	2.0	4 ± 1	0.5 ± 0.1
6	2.2	2.0	4.0 ± 0.9	0.1 ± 0.1
7	2.2	2.0	3.8 ± 0.9	0.10 ± 0.09

The residual errors (not showed in Table 4) were 0.13 and 0.31 for Group 1 and Group 2, respectively. While the pure errors (not showed in Table 4) estimated from the central points were the same (0.11) for both groups. These errors highlight the repeatability of the measurements.

In Figure 6 is shown the interaction plots of Frequency x Load (a) and Load x Frequency (b). From the results presented, it was possible to observe that:

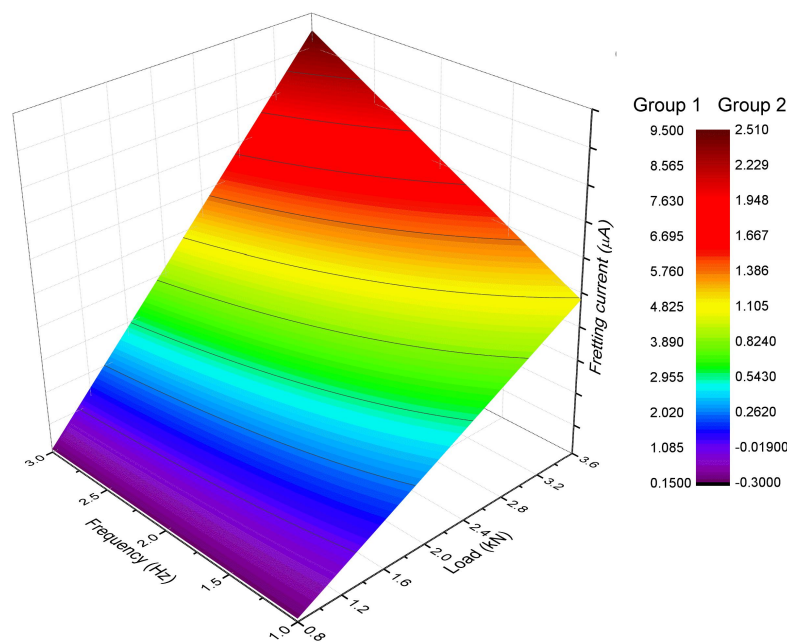
- Increasing the frequency has virtually no effect on the fretting corrosion on the minimum mechanical loading level, 0.8 kN (see Figure 6a).
- Increasing the loading level has a positive effect on fretting corrosion at both frequencies (see Figure 6b).
- For all prostheses, the highest fretting corrosion values were measured in the region of maximum load and frequency.
- At low level of loading (0.8 kN), the fretting corrosion current was zero, regardless of the frequency adopted for both groups.
- At high level of loading (3.6 kN) and low frequency (1.0 Hz) there was an increase in the fretting corrosion current to 4.6 ± 0.7 µA (Group1) and 0.9 ± 0.1 µA (Group 2).
- At high level of loading (3.6 kN) and high frequency (3.0 Hz) the fretting corrosion current increased (from Test N° 1 to Test N° 2) and practically doubled (9.3 ± 0.8 µA) for Group 1 and tripled (2.8 ± 0.1 µA) for Group 2.

Figure 6. Two way interaction plots: (a) Frequency x Load and (b) Load x Frequency.



By unifying these results in a surface plot, the effects of frequency and loading for both groups become clearly apparent (Figure 7). This surface allows us to identify trends between the levels of loading and frequency. Consequently, it was possible to predict the behavior of the implant under different levels of loading and frequency.

Figure 7. Surface plot of fretting corrosion currents.



For both groups, a cyclic loading of 0.8 kN did not induce an increase in fretting current, independent of the loading frequency. This occurs because the loading is not enough to cause significant rupture of the passive layer. Similar behavior has been identified in other studies, where the cyclic loading required to

initiate fretting corrosion varied between 0.5 and 2.2 kN, depending on the material combination (13-16). Regarding frequency, for both groups, an increase in frequency also results in an increase in fretting current. This is due to the competition between the rate of passive layer rupture and the formation of a new passive layer. Thus, an increase in the loading frequency affects the rate of wear and corrosion, leading to an increased corrosion rate (12).

To summarize, the measured currents were higher for Group 1, composed of dissimilar alloys between the stem and head (HNSS/CoCr). It is known that the mechanical and corrosion resistance for Co-Cr alloy is higher for CoCr implants followed by HNSS and lower for SS implants. Therefore, it was expected lower fretting corrosion current for pairs composed of more noble alloys as HNSS/CoCr. However, the results showed a different trend, in which was considered the possibility that the use of dissimilar alloys (between head and stem) could be increasing the fretting corrosion by adding a galvanic pair effect.

A greater fretting corrosion current is an indication that a greater release of ions and/or metallic particles has occurred. The greater release of these ions increases the potential to trigger an adverse tissue reaction, mainly due to the release of Co, Cr and Mo ions (6-8). These results highlighted the need to avoid combining modular implants composed of dissimilar alloys. It should be recommended both components made of the same alloy, CrCo for example, or a surface treatment as an option in terms of using stainless steel.

4. CONCLUSIONS

- The result of the central points (2.2 kN / 2.0 Hz) for all prostheses showed that the fretting corrosion tests presented good repeatability;
- The surface plot showed that, in all prostheses, the highest fretting corrosion values were in the region of maximum load and frequency;
- In both prostheses, fretting corrosion increased with increasing load from 0.8 kN to 3.6 kN, both at frequencies of 1.0 and 3.0 Hz;
- In both prostheses, there was no significant increase in fretting corrosion at the minimum load (0.8 kN) with the increase in frequency from 1.0 to 3.0 Hz.
- On the other hand, there was an increase in fretting corrosion with an increase in frequency from 1.0 to 3.0 Hz at maximum load (3.6 Hz);

- Group 1 (HNSS/CoCr) presented the highest fretting corrosion values;
- There is the possibility of galvanic corrosion contribution; however, the comparison is limited by the difference in geometric characteristics between the hip implants (connection design).

ACKNOWLEDGMENTS

The authors would like to thank CNPq for the financial support (postdoctoral research fellowships), and the National System of Nanotechnology Laboratories (MCTI/SisNANO/INT-CENANO-CNPq Process number 442604/2019-0).

REFERENCES

1. Wen C, Xiao G. Advances in osteoarthritis research in 2021 and beyond. *Journal of Orthopaedic Translation*. Epub ahead of print 2022. DOI: 10.1016/j.jot.2022.02.011.
2. Galia CR, Diesel CV, Guimarães MR, et al. Atualização em artroplastia total de quadril: uma técnica ainda em desenvolvimento. *Revista Brasileira de Ortopedia*. Epub ahead of print 2017. DOI: 10.1016/j.rbo.2016.09.013.
3. Kurtz SM, Lau E, Ong K, et al. Future young patient demand for primary and revision joint replacement: National projections from 2010 to 2030. In: *Clinical Orthopaedics and Related Research*. 2009. Epub ahead of print 2009. DOI: 10.1007/s11999-009-0834-6.
4. Callaghan JJ, Bracha P, Liu SS, et al. Survivorship of a Charnley total hip arthroplasty: A concise follow-up, at a minimum of thirty-five years, of previous reports. *Journal of Bone and Joint Surgery*. Epub ahead of print 2009. DOI: 10.2106/JBJS.H.01201.
5. Tan SC, Teeter MG, Del Balso C, et al. Effect of Taper Design on Trunnionosis in Metal on Polyethylene Total Hip Arthroplasty. *Journal of Arthroplasty* 2015; 30: 1269–1272.
6. Kwon YM, Tsai TY, Leone WA, et al. Sensitivity and Specificity of Metal Ion Levels in Predicting “Pseudotumors” due to Taper Corrosion in Patients With Dual Taper Modular Total Hip Arthroplasty. *Journal of Arthroplasty* 2017; 32: 996–1000.
7. Zhou Z, Liu X, Liu Q, et al. Evaluation of the potential cytotoxicity of metals associated with implanted biomaterials (I). *Preparative Biochemistry and*

Biotechnology 2009; 39: 81–91.

8. Li Y, Wong C, Xiong J, et al. Cytotoxicity of titanium and titanium alloying elements. *Journal of Dental Research*. Epub ahead of print 2010. DOI: 10.1177/0022034510363675.
9. Flores PB. Suscetibilidade à corrosão localizada em ligas utilizadas em implantes ortopédicos. Trabalho de Conclusão de Curso, Universidade Federal do Rio Grande do Sul.
10. Kurtz SM. UHMWPE Biomaterials Handbook: Ultra High Molecular Weight Polyethylene in Total Joint Replacement and Medical Devices. 2015. Epub ahead of print 2015. DOI: 10.1016/B978-0-323-35401-1.00042-9.
11. Shulman RM, Zywił MG, Gandhi R, et al. Trunnionosis: the latest culprit in adverse reactions to metal debris following hip arthroplasty. *Skeletal Radiology*. Epub ahead of print 2014. DOI: 10.1007/s00256-014-1978-3.
12. dos Santos VO, Cubillos PO, dos Santos CT, et al. Effect of Loading Frequency on the Fretting-Corrosion Degradation of the Stem-Head and Stem-Cement Interfaces in Hip Implants. *Journal of Testing and Evaluation*. Epub ahead of print 2024. DOI: 10.1520/JTE20220045.
13. Goldberg JR, Gilbert JL. In Vitro Corrosion Testing of Modular Hip Tapers. *Journal of Biomedical Materials Research - Part B Applied Biomaterials* 2003; 64: 78–93.
14. Rowan FE, Wach A, Wright TM, et al. The onset of fretting at the head-stem connection in hip arthroplasty is affected by head material and trunnion design under simulated corrosion conditions. *Journal of Orthopaedic Research* 2018; 36: 1630–1636.
15. Ouellette ES, Mali SA, Kim J, et al. Design, Material, and Seating Load Effects on In Vitro Fretting Corrosion Performance of Modular Head-Neck Tapers. *Journal of Arthroplasty*. Epub ahead of print 2019. DOI: 10.1016/j.arth.2019.01.043.
16. Pierre D, Swaminathan V, Scholl LY, et al. Effects of Seating Load Magnitude on Incremental Cyclic Fretting Corrosion in 5°40' Mixed Alloy Modular Taper Junctions. *Journal of Arthroplasty* 2018; 33: 1953–1961.